Vacuum 188 (2021) 110189

Contents lists available at ScienceDirect

Vacuum

journal homepage: http://www.elsevier.com/locate/vacuum

Dynamic behavior of clusters in the early stage of SiC (0001) epitaxial growth: A Kinetic Monte Carlo study

Xuejiang Chen [a,*], Wensen Ai [a], Hao Zhao [a], Yuan Li [b], Jianmei Feng [a]

[a] School of Energy and Power Engineering, Xi'an Jiaotong University, Xi'an, Shaanxi, 710049, PR China
[b] Department of Energy and Power Engineering, Qinghai Nationalities University, Xining, Qinghai, 810007, PR China

ARTICLE INFO

Keywords:
KMC
Early stage of nucleation
Silicon carbide
Clusters properties

ABSTRACT

A Kinetic Monte Carlo (KMC) model with a cluster-multiple labeling technique was proposed to study the effect of growth parameters such as temperature, deposition flux and Si/C ratio on Si–C clusters in the initial stage of SiC (0001) surface nucleation. In this model, Si and C atoms were treated individually and a crystal lattice was established to fix the physical location of atoms and interatomic bonding. The adsorption and diffusion of adatoms on the planar surface, attachment to and detachment from clusters of adatoms, and their diffusion along the edge of clusters were considered in the KMC model. Cluster-multiple labeling technique was used to identify Si–C clusters and the properties of clusters were analyzed. The results showed that larger and less clusters were constructed on growing surface with the increase of temperature and decrease of deposition rate. The saturated clusters density was exponentially related to the ratio of effective diffusion capacity to deposition rate, and the relationship between saturated density of clusters and average growth rate of clusters was obtained. Finally, Si/C ratio affected the characteristics of nucleation, and at C-rich condition, the binding energy of nucleus was larger than that at Si-rich condition, leading to the formation of fewer but larger clusters.

1. Introduction

Silicon carbide, a IV-IV compound material, is regarded as a promising semiconductor for power devices because of its wide band gap, high break-down voltage, high thermal conductivity, high saturation drift velocity and chemical inertness. Its exceptional physical and chemical properties make it possible to apply in high-power, high-frequency and high-temperature electronic devices [1,2]. Although development and progress have been achieved in crystal growth technology for SiC over the past several years, the relatively high densities of structure defects such as stacking fault, threading and misfit dislocations still severely hamper the widespread commercial application of SiC semiconductor device.

Epitaxial growth of SiC crystals can be obtained from the chemical vapor deposition (CVD) technique or molecular beam epitaxial (MBE) method. The growth of SiC epitaxial layers on low off-angle substrate was usually implemented in the CVD reactor under rough vacuum condition [3–9], and the operating pressure in MBE chamber was a typical ultra-high vacuum (UHV) [10–13]. In order to reduce the stacking faults and obtain single crystal epitaxial layers, step-controlled epitaxy was demonstrated by using a substrate with preprocessed steps [3,14], which led to the inheritance of specific polytype. Moreover, the formation mechanism of stepped morphologies have been revealed theoretically [15–17] and numerically [18–22]. It was found that it was difficult to achieve stable step-flow growth when the off-angle of substrate was less than 2° [16]. On the other hand, because of the observed reduction of defect density and the lower production cost [6,23–25], more attention has been paid on the epitaxial growth of SiC crystal on nearly on-axis substrate, which was also considered as one of the frontiers of SiC epitaxy [26].

Neudeck and Trunek obtained 3C–SiC growth with free of defects on planar 4H–SiC (0001) surface, while many screw dislocations were observed in 3C–SiC epitaxial layer on defective 4H–SiC substrate [5], which suggested that surface defects were the preferential nucleation sites. Kimoto and Matsunami experimentally investigated the effect of temperature and substrate polarity on nucleus density, and found that the nucleus density increased significantly with the decrease of temperature and it was higher on C face than on Si face [27]. Recently, considering the instability of different dimers, Ai proposed a set of coupled rate equations to study the nucleation process in the early stage of SiC epitaxial growth [28]. However, the microscopic behavior of silicon and carbon atoms can hardly be captured experimentally during

* Corresponding author.
E-mail address: xjchen@mail.xjtu.edu.cn (X. Chen).

https://doi.org/10.1016/j.vacuum.2021.110189
Received 6 January 2021; Received in revised form 29 January 2021; Accepted 8 March 2021
Available online 16 March 2021

SiC epitaxial growth, and the analytical model such as rate equations do not contain spatial correlations of clusters.

Kinetic Monte Carlo (KMC) simulation could provide a "real" solution to the thermally activated stochastic process. As an on-lattice model, KMC has been widely used in vacancy diffusion, grain growth and thin film growth [29–32]. For SiC epitaxial growth, Stout proposed an elaborate Monte Carlo surface kinetics model in which the transport of precursor to surface, diffusion, deposition, reaction and desorption of adatom were considered [18]. However, most of the KMC studies focused on step-flow growth mode [17–20,22] and the effect of nucleation on the stability of steps [21,33], and few researchers focused on the nucleation characteristics of silicon and carbon atoms on planar substrate during SiC epitaxial growth. Since clusters in the first layer form all the further growing [34], it is necessary to investigate the effect of the atomic-scale processes on the properties of Si–C clusters during the early stage of nucleation.

In this paper, a KMC simulation was carried out to study the dynamic behavior of Si–C clusters during the initial stage of epitaxial growth, and a cluster multiple labeling technique, also known as Hoshen - Kopelman algorithm [35], was applied to identify Si–C clusters. The effect of temperature and deposition rate on surface morphology was studied and the scaling relation of saturated density of clusters N_{st}, average growth rate of clusters R_{av} versus the ratio of effective diffusion capacity to deposition rate, namely D_{eff}/F, were also analyzed. Furthermore, the quantitative relationship between saturated density of clusters N_{st} and average growth rate of clusters R_{av} was obtained. Finally, the effect of Si/C ratio on the early stage of nucleation was investigated as well.

2. The model

In our KMC model, a single silicon or carbon atom is deposited randomly onto the empty surface site at a rate, F, and becomes adatom. Then it diffuses along the surface to their own neighboring sites in a random way. The adatoms could coalesce to form a cluster of size s ($s \geq 2$). Also the atoms on cluster perimeter could move along the edge of the cluster or detach from it, which means that the attachment of adatom to the cluster is reversible. Desorption is not permitted because of the much lower desorption rate than diffusion and deposition rate [20]. Furthermore, silicon or carbon monomers could only diffuse to their own neighbor sites, and are not allowed to jump up a layer. When clusters encounter, they will merge to become a larger one. Consequently, all of the events considered in this model are deposition, adatoms diffusion on the bare crystal surface, attachment to and detachment from clusters of adatoms, and their diffusion along the perimeter of clusters.

KMC simulation is carried out on the lattice mesh, in which the positions of particles and interatomic bonding are retained. Fig. 1 illustrates the neighbors of central silicon centered atom and top view of growth layer. Two kinds of bonds are considered, namely nearest neighbors (NN) and next nearest neighbors (NNN), respectively. NN bond refers to the bond between silicon and carbon atom and NNN bond corresponds to Si–Si or C–C bond. The effect of substrate layer on adatoms can be reflected by the diffusion barrier E_D, so the bonds between substrate layer and growth layer should not be counted in. For a given site on growth surface, the total number of bonds reaches nine, including three NN bonds and six NNN bonds.

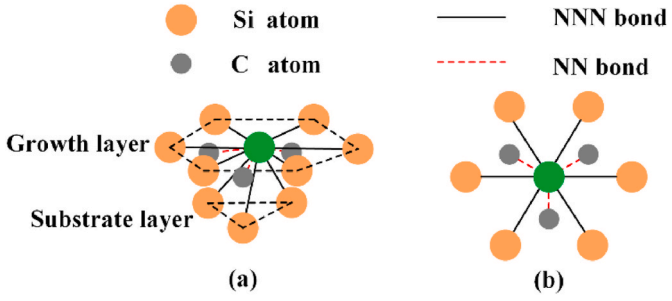

Fig. 1. (a) Neighbors of Si centered atom (green), brown and grey spheres depict Si and C atoms respectively. (b) Viewing in [0001] direction. Black solid lines and red dashed lines denote the bonds of next nearest and nearest neighbors.

The rate of diffusion event R_D depends on the substrate temperature T as well as the initial energy E_i and final energy E_f of hopping atom, and can be calculated as follows:

$$R_D = \nu_0 \exp\left(-\frac{\Delta E + E_D}{kT}\right) \tag{1}$$

where ν_0 is the attempt frequency which equals to 10^{10} ms^{-1}, k is Boltzmann's constant and T is substrate temperature. The activation barrier of surface diffusion E_D is set to 0.8eV and 1.1eV for Si and C atom, respectively [20]. ΔE is determined by the energy of initial and final site, written as:

$$\Delta E = \begin{cases} E_i - E_f & if \quad E_i > E_f \\ 0 & otherwise \end{cases} \tag{2}$$

The initial energy E_i and final energy E_f of hopping atom depend on the atom types and their local coordination which governed by occupied NN and NNN sites. Hence,

$$E_{i,f} = E_{Si-C}(n_{NN})_{i,f} + E_{Si-Si(C-C)}(n_{NNN})_{i,f} \tag{3}$$

where n_{NN} and n_{NNN} are the occupancy of NN and NNN neighbors, respectively. And $E_{Si-C} = 0.75$eV, $E_{Si-Si} = 0.35$eV, $E_{C-C} = 0.65$eV [17, 19–22].

Although the height of silicon and carbon atoms in growth layer are not same, we analyze the clusters composed of Si and C atoms rather than Si–Si or C–C clusters. The process of cluster identification starts from the original site of growth layer, then goes through each lattice column by column and layer by layer. For the lattice site occupied by Si or C atom will be assigned a cluster label α which will also assign to the unlabeled neighbors of the occupied site. However, if the neighbors have already been named a cluster label β, the proper cluster label must be determined. Therefore, Hoshen- Kopelman algorithm is applied to solve this problem and more details can be found in Ref. [35].

3. Result and discussion

Both diffusion rate D and deposition rate F of adatoms are important parameters that determine the dynamic behavior of epitaxial nucleation growth at the early stage. In this work, the temperature of substrate is varied from 1000K to 1500K, and the deposition rate is in the range of F = 0.01–0.5 ms^{-1}. The size of simulation box is 115 × 200 × 4. Considering the high symmetry of configuration, orientations of $[10\bar{1}0]$ and $[11\bar{2}0]$ are chosen as the directions for the two sides of simulation cell, in which the periodic boundary conditions are applied.

3.1. Morphology of growing surface

Fig. 2 presents a top view of the nucleation growth produced by the KMC simulations, where the brown and black spheres represent Si and C atoms on growing surface, respectively. The terminated Si particles on the substrate towards the (0001) surface are represented by blue spheres. Morphologies for six different temperatures at F=0.1 ms^{-1} and coverage of θ = 0.1 ML are shown in Fig. 2 (a). It can be seen that the number of Si–C clusters gradually decreases with the increase of substrate temperature, and that the average size of Si–C clusters at high temperature is much larger than that at low temperature. In addition, the shape of Si–C clusters becomes more compact at higher temperatures. The movement of Si and C atoms on the substrate is thermally activated and a higher temperature corresponds to a larger diffusion

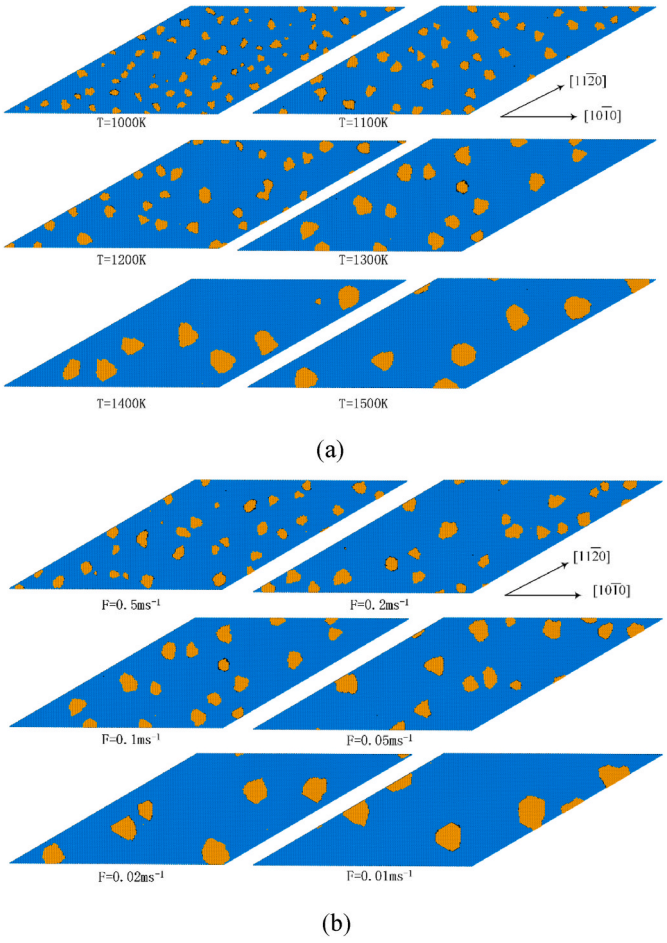

Fig. 2. Morphologies of growing surfaces for (a) various temperatures at $F = 0.1$ ms^{-1} and (b) various deposition rates at $T = 1300$K. The coverage is 0.1 ML and the size of computational box is 115 × 200 × 4. The substrate Si atoms are shown in blue, and the Si and C atoms on growing surfaces are represented by brown and black spheres, respectively.

capacity and diffusion length of adatoms. Therefore, adatoms tend to coalesce to form larger and more stable clusters in the same interval of deposition. Fig. 2 (b) demonstrates morphologies for various deposition rates at $T = 1300$K and coverage of $\theta = 0.1$ ML. From Fig. 2 (b), we can find that fewer Si–C clusters with larger size are obtained by decreasing the deposition rate at a fixed temperature. But the evolution mechanism of Si–C clusters in Fig. 2 (b) is totally different from that in Fig. 2 (a). At a given temperature, the diffusion rate of adatom is constant and the decrease of deposition rate indicates the increase of interval between each deposition. Thus, adatoms have enough time to aggregate to form a larger cluster or attach to existing clusters before the next deposition. Although the evolution mechanism in Fig. 2 (a) and 2(b) are different, their evolution characteristics are similar. Therefore, increasing substrate temperature or decreasing deposition rate, in other words, a large ratio of diffusion to deposition rate is beneficial to the formation of larger islands, which is in accord with the experimental observation [27] and theoretical analysis [36].

3.2. Analysis of Si–C cluster properties

To investigate the formation and evolution of Si–C clusters during the initial stage of nucleation, some cluster properties are quantitatively analyzed. Fig. 3 shows the relationship between cluster density and temperature and deposition rate in the early stage of nucleation, which is a function of coverage. As shown in the figure, the density of clusters is

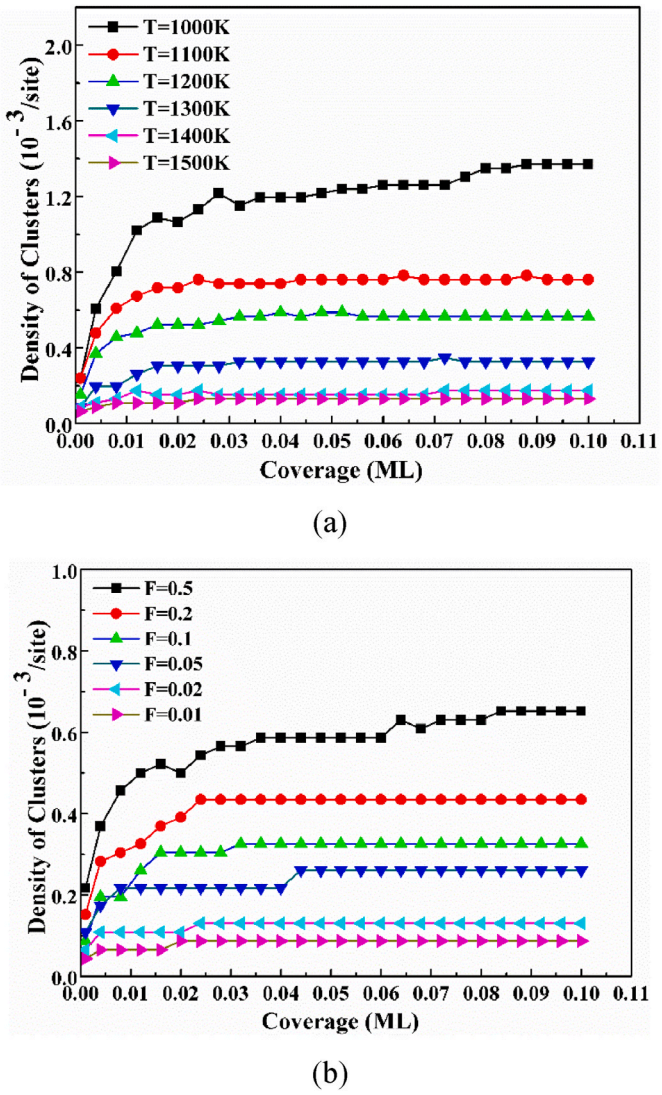

Fig. 3. Number density of clusters versus coverage for (a) various temperatures at $F = 0.1$ ms^{-1} and (b) various deposition rates at $T = 1300$K

decreased with the increase of temperature and decrease of deposition rate within the coverage of 0.1 ML. In Fig. 3 (a), it can be seen that the growth rate of clusters density decreases with the increase of substrate temperature within the coverage of 0.01 ML and the clusters density becomes saturated after coverage reaches 0.02 ML. Fig. 3 (b) demonstrates that the increase rate of clusters density decreases with the descending of deposition rate at low coverage (within 0.01 ML) and the density of clusters also becomes saturated for all cases at high coverage. Additionally, the saturated density of Si–C clusters also decreases with the ascending of temperature and descending of deposition rate, which corresponds to the morphology results in Fig. 2 (a) and 2(b). Therefore, the density of clusters is negatively correlated with temperature, while clusters density is positively correlated with deposition rate.

For Si–C binary component system, the diffusion rate of each species is not equal due to the different diffusion activation barrier. Therefore, combining the diffusion rate of Si and C atoms, an effective diffusion rate [37] is defined to describe the diffusion capacity of the system:

$$D_{eff}{}^{-1} = m_{Si} D_{Si}{}^{-1} + m_C D_C{}^{-1} \quad (4)$$

where m_{Si} and m_C are mole fractions of silicon and carbon atoms in the flux and are set to 0.5, which indicates that the deposition probability for Si and C atoms is equal. To find out the relationship between Si–C

clusters density and D_{eff}/F, the saturated number density of clusters N_{st} is defined, which is the average value of clusters density from θ= 0.08 ML to θ=0.1 ML in Fig. 3. Fig. 4 shows the relationship between N_{st} and D_{eff}/F for temperatures from 1000K to 1500K at F = 0.1 ms^{-1} (black squares) and for deposition rates from 0.01 to 0.5 ms^{-1} at T = 1300K (red circles). And, the red solid line in the figure is the power fit of saturated density of clusters versus D_{eff}/F, with the exponent of −0.499 ± 0.001. It can be clearly observed that N_{st} decreases with the increase of D_{eff}/F. Thus we obtain

$$N_{st} \sim \left(D_{eff}/F\right)^{\gamma} \delta\gamma = -0.499 \pm 0.001 \tag{5}$$

Fig. 5 shows the dependence of temperature and deposition rate on the average size of clusters (monomers excluded) during the early stage of nucleation. As circled in Fig. 5, there are some fluctuations of the data, which is mainly due to the formation of new clusters, and this could slightly reduce the average size of Si–C clusters. The results show that the growth rate of Si–C clusters increases with the increase of temperature and decrease of deposition rate, and the average size of clusters grows linearly with the increase of the coverage at different temperatures and deposition rates.

In order to figure out the quantitative relationship between average size of clusters and D_{eff}/F, the average growth rate of clusters R_{av} is defined, which equals to the derivative of average size of clusters to coverage.

$$R_{av} = \left(S_{av}\right)' = dS_{av}/d\theta \tag{7}$$

Fig. 6 illustrates the relationship between R_{av} and D_{eff}/F for temperatures from 1000K to 1500K at F = 0.1 ms^{-1} (black squares) and for deposition rates from 0.01 to 0.5 ms^{-1} at T = 1300K (red circles). The red solid line in the figure is the power fit of average growth rate of clusters versus D_{eff}/F, with the exponent of 0.505 ± 0.002. It can be seen that R_{av} increases with the increase of D_{eff}/F, and we can obtain that

$$R_{av} \sim \left(D_{eff}/F\right)^{\gamma'} \tag{8}$$

As the value of $-\gamma = 0.499 \pm 0.001$ in Eq. (5) and the exponent $\gamma' = 0.505 \pm 0.002$ in Eq. (8)are very close, the relationship between average growth rate of clusters and saturated number density of clusters can be obtained from Eqs. (5) and (8):

$$R_{av} \sim \left(N_{st}\right)^{-1} \tag{9}$$

The result indicates that R_{av} and N_{st} are dependent and inversely proportional, which is consistent with the prediction results by scale theory under the condition that the density of clusters is much larger

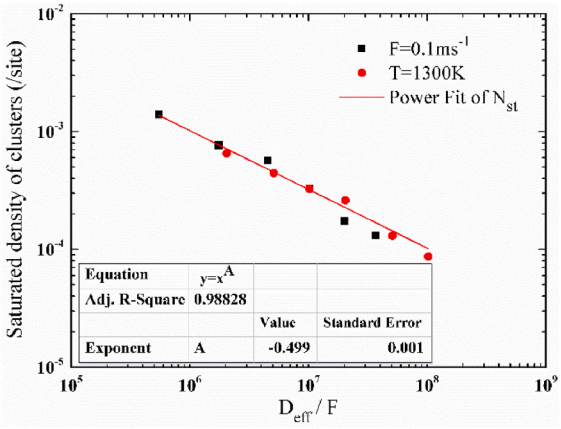

Fig. 4. Saturated density of clusters N_{st} as a function of D_{eff}/F. Black squares represent T = 1000–1500K at F = 0.1 ms^{-1}, and red circles represent F = 0.01–0.5 ms^{-1} at T = 1300K. Red solid line is the power fit of N_{st} with exponent of −0.499 ± 0.001.

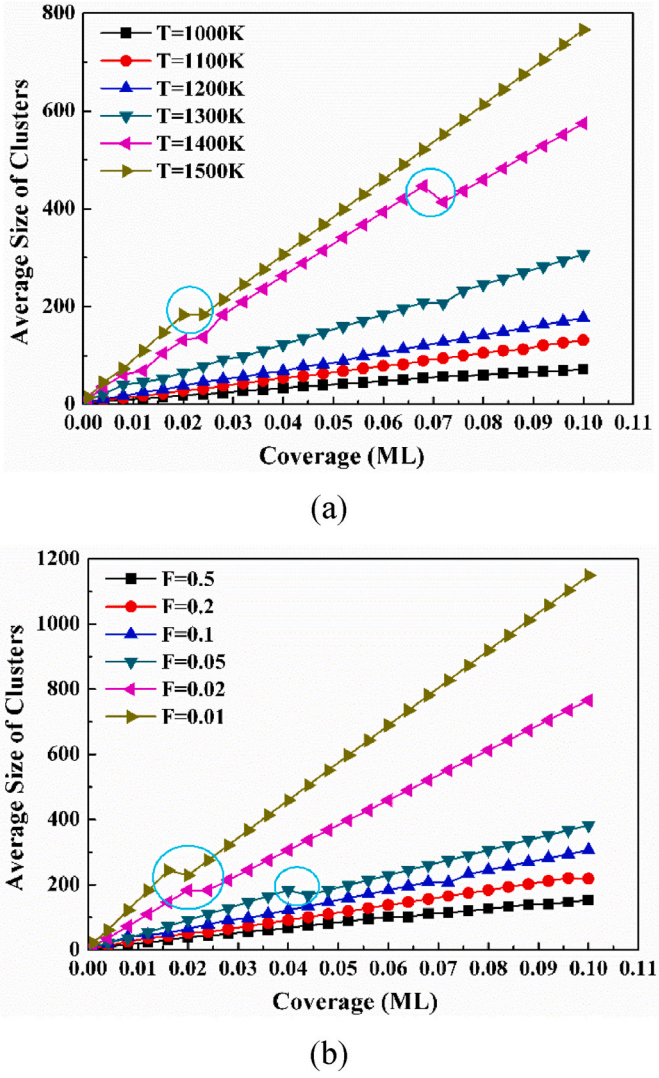

Fig. 5. Average size of clusters versus coverage for (a) different temperatures at F = 0.1 ms^{-1} and (b) different deposition rates at T = 1300K

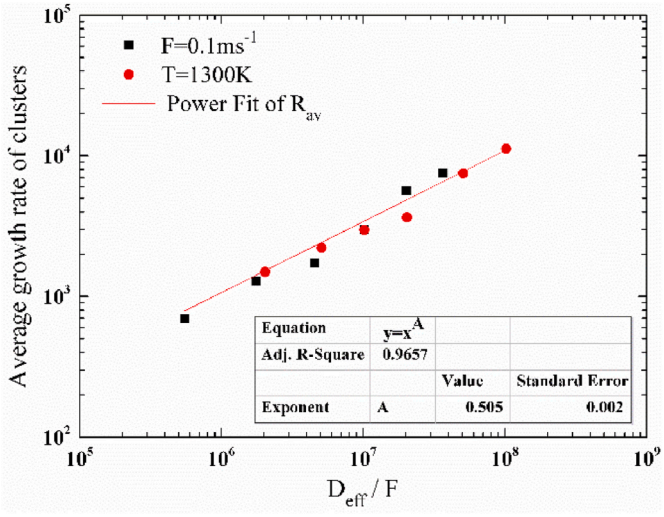

Fig. 6. Average growth rate of clusters R_{av} as a function of D_{eff}/F. Black squares represent T = 1000–1500K at F = 0.1 ms^{-1}, and red circles represent F = 0.01–0.5 ms^{-1} at T = 1300K. Red solid line is the power fit of R_{av} with exponent of 0.505 ± 0.002.

than that of monomers [34]. Therefore, the higher the value of D_{eff}/F is, the higher average growth rate of clusters is and the lower density of clusters is at the same coverage range, which is beneficial to the initial stage of epitaxial nucleation of SiC.

3.3. Effect of Si/C ratio on nucleation of early stage

The Si/C ratio on the growing surface has a significant effect on surface morphologies [4,8,9,25]. In experiments, the Si/C ratio was controlled by varying the flow rate of gas source, and a more regular surface morphology of 4H–SiC (0001) Si-face epitaxial layer was obtained at C/Si = 0.6 than at C/Si = 1.5 by Kojima [4]. Nakamura reported that a C/Si ratio of 2 in the gas flow was beneficial to the homoepitaxial growth on nearly on-axis 6H–SiC (0001) substrate [25]. However, the microscopic mechanism is still unclear at present. Therefore, the effect of deposited Si/C ratio on the early stage of SiC (0001) surface epitaxial growth is discussed.

In our KMC model, the modification of Si/C ratio is achieved by changing the mole fraction of Si and C atoms in deposition flux. The mole fraction of Si atom, m_{Si}, ranges from 0.6 to 0.3 and the mole fraction of C atom, m_C, is accordingly varied from 0.4 to 0.7. Fig. 7 shows the morphologies of growing surfaces for different Si/C ratios at T = 1300K, $F = 0.1$ ms^{-1} and coverage of $\theta = 0.1$ ML, where the blue, brown and black spheres represent Si-termination substrate, Si and C atoms of growing surface, respectively. It can be seen that Si/C ratio significantly affects the density of Si–C clusters and the clusters density at Si-rich condition is larger than that at C-rich condition. Moreover, with the increase of m_C, the shape of clusters becomes more compact and the average size of clusters becomes larger. Therefore, the higher concentration of C in deposition flux is beneficial to the early stage of nucleation.

Fig. 8 demonstrates the relationship between N_{st} and D_{eff}/F for different Si/C ratios, varying T from 1000K to 1500K at $F = 0.5$ ms^{-1} (black squares), 0.1 ms^{-1} (red circles) and 0.01 ms^{-1} (blue triangles), respectively. The red solid lines are the power fit of saturated density of clusters N_{st} versus D_{eff}/F, with the exponents of $\gamma_{6/4} = -0.483 \pm 0.002$, $\gamma_{5/5} = -0.506 \pm 0.002$, $\gamma_{4/6} = -0.502 \pm 0.002$ and $\gamma_{3/7} = -0.525 \pm 0.002$, respectively. It can be observed that the exponent changes with the Si/C ratio, which indicates that Si/C ratio affects the critical nucleation of Si–C clusters. As mentioned in Section 2, the energy of Si–Si bond (0.35eV) is smaller than that of Si–C (0.75eV) and C–C bond (0.65eV). As the Si/C ratio is 6/4 (corresponding to $m_{Si} = 0.6$ and $m_C = 0.4$), which is a Si-rich condition, there are more Si–Si bonds but less Si–C and C–C bonds than that at the condition of $m_{Si} = 0.5$ and $m_C = 0.5$. Moreover, the exponent of $\gamma_{6/4}$ is larger than that of $\gamma_{5/5}$, which indicates that the increment of binding energy caused by the increase of Si–Si bonds cannot afford the energy decrement caused by the decrease of Si–C and C–C bonds, leading to the formation of nucleus with a smaller binding energy. As a result, the capacity of capturing adatoms of the cluster becomes weak, which leads to the tendency that the atoms locating at the perimeter detach from the clusters and more clusters are formed under the condition of Si-rich. And as Si/C ratio is 4/6 (corresponding to $m_{Si} = 0.4$ and $m_C = 0.6$), which is a C-rich condition, fewer Si–Si and Si–C bonds but more C–C bonds are formed. Note that the exponent of $\gamma_{4/6}$ and $\gamma_{5/5}$ are similar and close to −0.5, which suggests that the increase of binding energy caused by the increase of C–C bonds almost counteracts the decrease of energy caused by the decrease of Si–Si and Si–C bonds. With the further increasing of mole fraction of C atom, $m_{Si} = 0.3$ and $m_C = 0.7$, the exponent of $\gamma_{3/7}$ decreases to -0.525 ± 0.002 and is smaller than that of $\gamma_{5/5}$ and $\gamma_{4/6}$, which denotes that the increase of binding energy caused by the further increase of C–C bonds overwhelms the energy decrease of the system caused by the further decrease of Si–C and Si–Si bonds, which leads to the formation of nucleus with a larger binding energy. Therefore, for a C-richer condition, the clusters are more stable and adatoms tend to attach to rather than detach from the clusters, resulting in the formation of fewer but larger clusters, which corresponds to the morphology results in Fig. 7.

4. Conclusion

The dynamic characteristics of clusters in the early stage of SiC (0001) surface epitaxial growth has been investigated by Kinetic Monte Carlo method and Hoshen- Kopelman algorithm. The morphology results indicate that larger and less clusters are formed on the substrate by increasing the temperature and decreasing the deposition rate at coverage of $\theta = 0.1$ ML. For $F = 0.1$ ms^{-1}, the growth rate of Si–C clusters density decreases with the increase of temperature and the clusters density has been saturated after coverage reaches 0.02 ML. For T = 1300K, the growth rate of clusters density increases with the increase of deposition rate at low coverage and the density of clusters also becomes saturated at high coverage. The saturated density of clusters N_{st} is exponentially related to D_{eff}/F, and the index, γ, equals to -0.499 ± 0.001. Moreover, the inverse proportional relationship between saturated density of clusters N_{st} and average growth rate of clusters R_{av} is obtained, which is in good agreement with the prediction of scaling theory. Finally, Si/C ratio has an effect on morphology of growing surface and density of clusters. For C-rich condition, less and more compact clusters are obtained. Si/C ratio also affects the critical nucleation of Si–C clusters, and at Si-rich condition, the binding energy of nucleus is smaller than that at C-rich condition. With the further increase of mole fraction of C atom, $m_{Si} = 0.3$ and $m_C = 0.7$, the binding energy of nucleus becomes larger, which results in the formation of fewer but larger

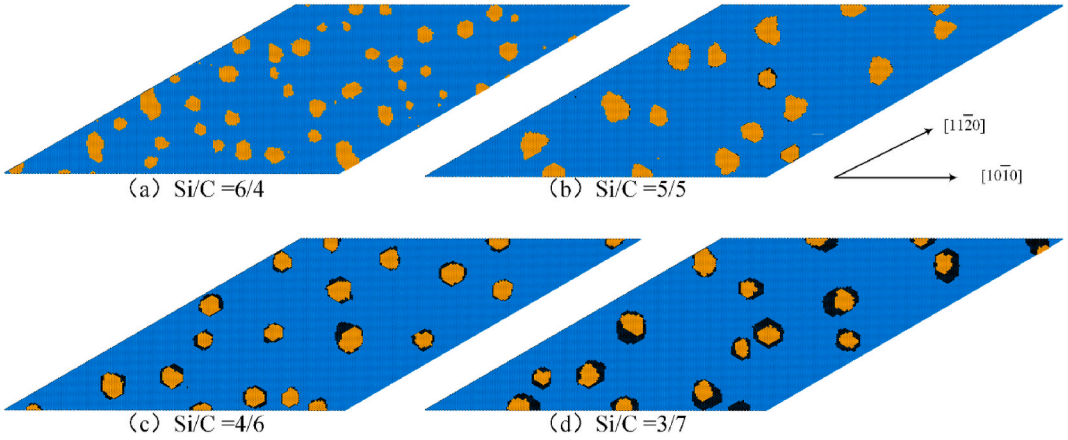

Fig. 7. Morphologies of growing surfaces for various Si/C ratios at T = 1300K and $F = 0.1$ ms^{-1}. The coverage is 0.1 ML and the size of computational box is 115 × 200 × 4. The substrate Si atoms are shown in blue, and the Si and C atoms on growing surfaces are represented by brown and black spheres, respectively.

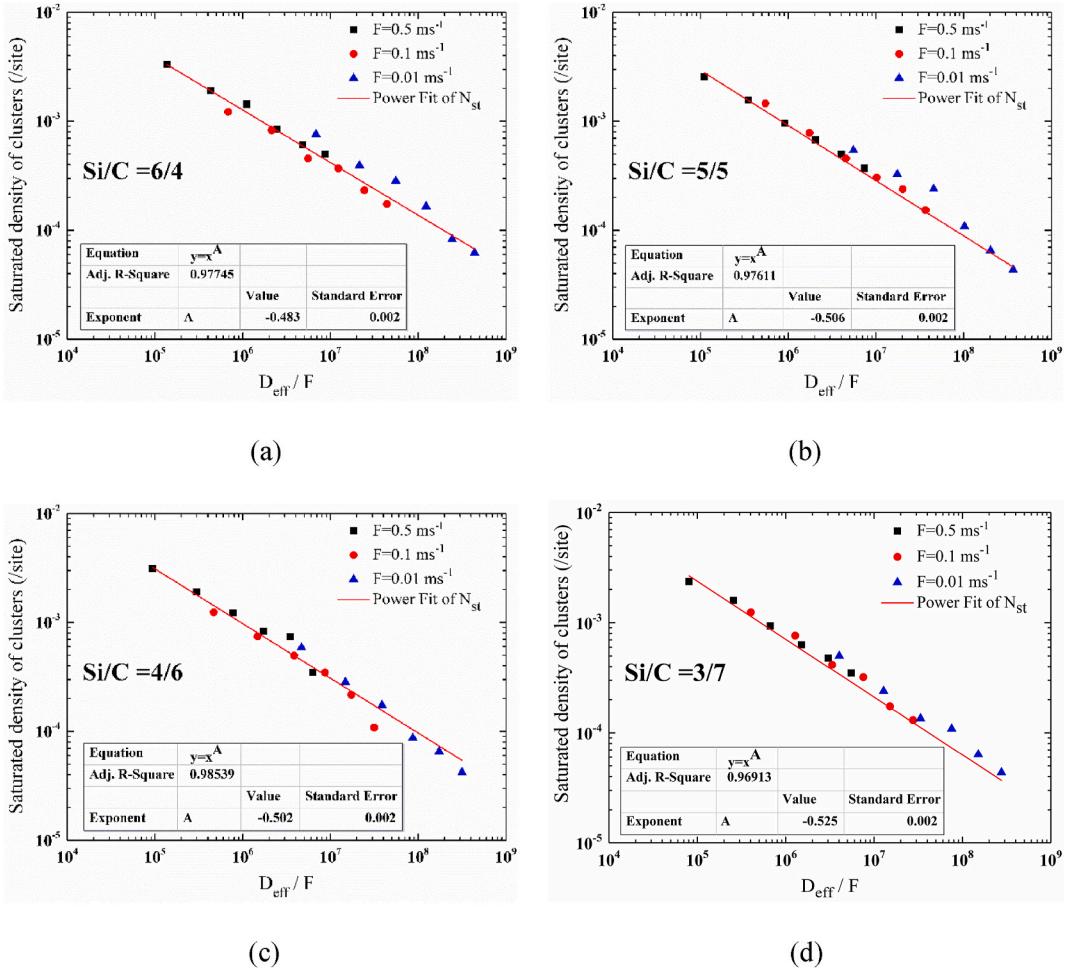

Fig. 8. Saturated density of clusters N_{st} as a function of D_{eff}/F for various Si/C ratios. Black squares, red circles and blue triangles represent $T = 1000$–1500K at $F = 0.5$ ms^{-1}, $F = 0.1$ ms^{-1} and $F = 0.01$ ms^{-1}, respectively. Red solid lines are the power fit of N_{st} with exponents of $\gamma_{6/4} = -0.483 \pm 0.002$, $\gamma_{5/5} = -0.506 \pm 0.002$, $\gamma_{4/6} = -0.502 \pm 0.002$ and $\gamma_{3/7} = -0.525 \pm 0.002$, respectively.

clusters.

Declaration of competing interest

The authors declare that they have no known competing financial interests or personal relationships that could have appeared to influence the work reported in this paper.

References

[1] T. Kimoto, Material science and device physics in SiC technology for high-voltage power devices, Jpn. J. Appl. Phys. 54 (2015), 040103.

[2] H. Matsunami, Technological breakthroughs in growth control of silicon carbide for high power electronic devices, Jpn. J. Appl. Phys. 43 (2004) 6835–6847.

[3] H.S. Kong, J.T. Glass, R.F. Davis, Chemical vapor deposition and characterization of 6H-SiC thin films on off-axis 6H-SiC substrates, J. Appl. Phys. 64 (1988) 2672–2679.

[4] K. Kojima, H. Okumura, S. Kuroda, K. Arai, Homoepitaxial growth of 4H-SiC on on-axis C-face substrates by chemical vapor depositon, J. Cryst. Growth 269 (2004) 367–376.

[5] P.G. Neudeck, A.J. Trunek, D.J. Spry, J.A. Powell, H. Du, M. Skowronski, X. R. Huang, M. Dudley, CVD growth of 3C-SiC on 4H/6H mesas, Chem. Vap. Depos. 12 (2006) 531–540.

[6] S. Leone, H. Pedersen, A. Henry, O. Kordina, E. Janzén, Thick homoepitaxial layers grown on on-axis Si-face 6H- and 4H-SiC substrates with HCl addition, J. Cryst. Growth 312 (2009) 24–32.

[7] K. Masumoto, H. Asamizu, K. Tamura, C. Kudou, J. Nishio, K. Kojima, T. Ohno, H. Okumura, Homoepitaxial growth and investigation of stacking faults of 4H-SiC C-face epitaxial layers with a 1° off-angle, Jpn. J. Appl. Phys. 54 (2015), 04DP04.

[8] A. Balachandran, H. Song, T.S. Sudarshan, M.V.S. Chandrashekhar, 4H–SiC homoepitaxy on nearly on-axis substrates using TFS-towards high quality epitaxial growth, J. Cryst. Growth 448 (2016) 97–104.

[9] Z. Zhao, Y. Li, X. Xia, Y. Wang, P. Zhou, Z. Li, Growth of high-quality 4H-SiC epitaxial layers on 4° off-axis C-face 4H-SiC substrates, J. Cryst. Growth 531 (2020) 125355.

[10] S. Motoyama, S. Kaneda, Low-temperature growth of 3C-SiC by the gas source molecular beam epitaxial method, Appl. Phys. Lett. 54 (1989) 242–243.

[11] L.B. Rowland, R.S. Kern, S. Tanaka, R.F. Davis, Gas-source molecular beam epitaxy of monocrystalline β–SiC on vicinal α(6H)–SiC, J. Mater. Res. 8 (1993) 4.

[12] A. Fissel, B. Schröter, W. Richter, Low-temperature growth of SiC thin films on Si and 6H–SiC by solid-source molecular beam epitaxy, Appl. Phys. Lett. 66 (1995) 3182–3184.

[13] A. Fissel, U. Kaiser, J. Kraußlich, K. Pfennighaus, B. Schroter, J. Schulz, W. Richter, Epitaxial growth of SiC-heterostructures on α-SiC(0001) by solid-source MBE, Mater. Sci. Eng., B 61–62 (1999) 4.

[14] T. Kimoto, A. Itoh, H. Matsunami, Step bunching in chemical vapor deposition of 6H– and 4H–SiC on vicinal SiC(0001) faces, Appl. Phys. Lett. 66 (1995) 3645–3647.

[15] T. Kimoto, H. Nishino, W.S. Yoo, H. Matsunami, Growth mechanism of 6H-SiC in step-controlled epitaxy, J. Appl. Phys. 73 (1993) 726–732.

[16] T. Kimoto, H. Matsunami, Surface kinetics of adatoms in vapor phase epitaxial growth of SiC on 6H-SiC{0001} vicinal surfaces, J. Appl. Phys. 75 (1994) 850–859.

[17] Y. Li, X. Chen, J. Su, Study on formation of step bunching on 6H-SiC (0001) surface by kinetic Monte Carlo method, Appl. Surf. Sci. 371 (2016) 242–247.

[18] P.J. Stout, Modeling surface kinetics and morphology during 3C, 2H, 4H, and 6H–SiC, J. Vac. Sci. Technol., A 16 (1998) 15.

[19] V. Borovikov, A. Zangwill, Step bunching of vicinal6H-SiC{0001}surfaces, Phys. Rev. B 79 (2009) 245413.

[20] F. Krzyżewski, M.A. Załuska–Kotur, Coexistence of bunching and meandering instability in simulated growth of 4H-SiC(0001) surface, J. Appl. Phys. 115 (2014) 213517.

[21] Y. Li, X. Chen, J. Su, Effect of nucleation on instability of step meandering during step-flow growth on vicinal 3C-SiC (0001) surfaces, J. Cryst. Growth 468 (2017) 28–31.
[22] X. Chen, Y. Li, Stepped morphology on vicinal 3C- and 4H-SiC (0001) faces: a kinetic Monte Carlo study, Surf. Sci. 681 (2019) 18–23.
[23] J. Hassan, J.P. Bergman, A. Henry, E. Janzén, On-axis homoepitaxial growth on Si-face 4H–SiC substrates, J. Cryst. Growth 310 (2008) 4424–4429.
[24] W. Chen, M.A. Capano, Growth and characterization of 4H-SiC epilayers on substrates with different off-cut angles, J. Appl. Phys. 98 (2005) 114907.
[25] S. Nakamura, T. Kimoto, H. Matsunami, Homoepitaxy of 6H–SiC on nearly on-axis (0001) faces by chemical vapor deposition Part I: effect of C/Si ratio on wide-area homoepitaxy without 3C–SiC inclusions, J. Cryst. Growth 256 (2003) 341–346.
[26] T. Kimoto, Bulk and epitaxial growth of silicon carbide, Prog. Cryst. Growth Char. Mater. 62 (2016) 329–351.
[27] T. Kimoto, H. Matsunami, Nucleation and step motion in chemical vapor deposition of SiC on 6H-SiC{0001} faces, J. Appl. Phys. 76 (1994) 7322–7327.
[28] W. Ai, X. Chen, Y. Li, H. Zhao, Application of self-consistent rate equations approach for SiC (0001) surface epitaxial growth, Comput. Mater. Sci. 188 (2021) 110253.
[29] A. Chatterjee, D.G. Vlachos, An overview of spatial microscopic and accelerated kinetic Monte Carlo methods, J. Comput. Aided Mater. Des. 14 (2007) 253–308.
[30] C.C. Battaile, The Kinetic Monte Carlo method: foundation, implementation, and application, CMAME 197 (2008) 3386–3398.
[31] I. Martin-Bragado, R. Borges, J.P. Balbuena, M. Jaraiz, Kinetic Monte Carlo simulation for semiconductor processing: a review, Prog. Mater. Sci. 92 (2018) 1–32.
[32] S. Blel, A.B.H. Hamouda, Formation of Ag and Co nanowires at the step of the Cu (100) vicinal surfaces: a kinetic Monte Carlo study, Vacuum 151 (2018) 133–139.
[33] F. Krzyżewski, 4H-SiC surface structure transitions during crystal growth following bunching in a fast sublimation process, J. Cryst. Growth 401 (2014) 511–513.
[34] G.S. Bales, D.C. Chrzan, Dynamics of irreversible island growth during submonolayer epitaxy, Phys. Rev. B 50 (1994) 6057–6067.
[35] R.K. Hoshen, Percolation and cluster distribution. I. Cluster multiple labeling technique and critical concentration algorithm, Phys. Rev. B 14 (1976) 3438–3445.
[36] T. Kimoto, H. Matsunami, Surface diffusion lengths of adatoms on 6H-SiC{0001} faces in chemical vapor deposition of SiC, J. Appl. Phys. 78 (1995) 3132–3137.
[37] M. Einax, S. Ziehm, W. Dieterich, P. Maass, Scaling of island densities in submonolayer growth of binary alloys, Phys. Rev. Lett. 99 (2007), 016106.